Journal of Materials Chemistry A

PAPER

Check for updates

Cite this: J. Mater. Chem. A, 2018, 6, 23638

Topotactic conversion of calcium carbide to highly crystalline few-layer graphene in water†

Yin Jia,[ab] Xiangchao Chen,[c] Guoxin Zhang,*[c] Lin Wang,[a] Cejun Hu[b] and Xiaoming Sun*[abc]

Received 5th September 2018
Accepted 24th October 2018

DOI: 10.1039/c8ta08632j

rsc.li/materials-a

The reaction of calcium carbide (CaC_2) with water to produce acetylene is common in industrial production, but its side reaction, removal of calcium from CaC_2 (also termed de-Ca) to fabricate highly graphitic carbon, is highly overlooked. Herein, we report the synthesis of highly crystalline few-layered graphene by controlling the reaction of tetragonal-phased CaC_2 with water at room temperature (20–25 °C). The resulting carbon materials were revealed to be highly graphitic, with ~3 nm thickness, containing >93 at% carbon. Raman spectroscopy evidenced their low defect content with a defect (D)/graphitization (G) ratio of ~0.07. HRTEM further verified their high graphitization degree. A formation mechanism was proposed: the C_2^{2-} dumbbells donate their electrons to nearby oxidative species, *e.g.* H^+ in water, followed by topotactic cross-linking to form a conjugated sp^2-carbon network. Furthermore, the capability of CaC_2 reduction and re-assembly into graphitic carbon was clearly evidenced by reaction with Ag^+ in non-aqueous solvent, which resulted in a larger quantity of graphene materials and small-sized Ag nanoparticles.

1. Introduction

Graphene, the atomically-thin layered allotrope of carbon, has received tremendous attention and enabled the dramatic advance of electronics over the last decade due to its unprecedented physical properties.[1–4] To realize its excellent physical properties, subtly controlling the crystallinity and defect content is a prerequisite.[5–7] Initially, mechanical cleavage methods (including the Scotch tape method[8] and exfoliating graphite in solvents[9–12]) of natural graphite were applied to obtain high-quality graphene materials due to the ease of operation; however, these methods can hardly afford scalable graphene production. Thereafter, chemical vapor deposition that is capable of synthesizing defect-free graphene (DFG) on a large scale through chemical routes was developed; however, high temperature (usually 900–1100 °C) and catalytic substrates (such as Ni, Cu, *etc.*) are often required.[13–15] It was previously reported that graphitic carbon could be synthesized at around 220–250 °C by effectively breaking the C–Br bonds of hexabromobenzene precursors; however, the defect content was pronounced, which is unsatisfactory.[16] Therefore, synthesizing DFG under mild conditions (such as temperature ~ 20–25 °C) remains highly challenging.

Carbides represent a typical source for carbon fabrication.[17] A few stable carbides such as SiC, TiC, and B_4C have been vastly investigated as carbon sources, and assisted by chlorine or hydrogen chloride, highly porous amorphous carbon materials are obtainable.[18–21] Most recently, a facile redox method to convert Li_2C_2 (in the orthorhombic phase) into a patterned carbon containing periodic sp^2 and sp^3 domains under mild conditions (<80 °C) was reported by Paul Simon *et al.*, and it was mainly facilitated by the effective electron extraction from C_2^{2-} anions by oxidative Sn^{4+}.[22] It was also observed that adjacent C_2^{2-} anions in Li_2C_2 exhibit strong coupling when Li^+ was electrochemically extracted from the Li_2C_2 lattice, leading to the formation of the C≡C···C≡C linear form of carbon.[23] Although high-temperature treatment of the carbonaceous materials obtained from Li_2C_2 at low temperatures is still needed to obtain a high graphitization degree,[18,24] such redox-chemistry-based approaches show us that metal carbides support the fabrication of graphitic carbon materials or even graphene under mild conditions. However, alkaline metal carbides such as Li_2C_2 are extremely sensitive to moisture and oxygen, which creates a strong barrier for a comprehensive investigation.[25–27]

Calcium carbide (CaC_2), a widely available alkaline earth metal carbide that has many critical industrial applications (especially the formation of acetylene through reaction with water),[26,28] is much more stable than Li_2C_2. CaC_2 also belongs to

[a]State Key Laboratory of Chemical Resource Engineering, Beijing Advanced Innovation Center of Soft Materials Science and Engineering, Beijing University of Chemical Technology, Beijing 100029, China. E-mail: sunxm@mail.buct.edu.cn

[b]College of Energy, Beijing University of Chemical Technology, Beijing 100029, China

[c]College of Electrical Engineering and Automation, Shandong University of Science and Technology, Qingdao 266590, China. E-mail: zhanggx@sdust.edu.cn

† Electronic supplementary information (ESI) available: Further details of FLG synthesized using LiOH, acetic acid, ethylene glycol, and $AgNO_3$/NMP solution, including SEM images, XRD profiles, and Raman spectra. See DOI: 10.1039/c8ta08632j

the family of carbide compounds known as acetylides, which can be regarded as salts with C_2^{2-} anions. Interestingly, there have been previous reports revealing that the C_2^{2-} anions in CaC_2 can approach each other or even self-polymerize at high pressures (~7 GPa).[29–32] Because of the commercial importance of acetylene, numerous investigations have been focused on the reaction with water to form acetylene and calcium hydroxide.[33–36] Normally, at relatively low temperatures, this reaction likely follows formula (1) or (2) to give acetylene, but at high temperatures, carbon and hydrogen instead of acetylene can be formed (formula (3)), which is barely acknowledged.[35] Given the redox chemistry occurring in Li_2C_2 research, the formation of carbon at high temperatures is possibly *via* the coupling of C_2^{2-} anions. However, it is known that the reaction of CaC_2 with water to form carbon and H_2 is exothermic ($\Delta G_m^\theta = -86.6$ kJ mol^{-1}), meaning that this reaction can occur under common reaction conditions. Considering its favourable thermodynamics, we are confident that by exploring dynamically feasible routes, CaC_2 can result in graphitic carbon or even graphene under mild conditions by reacting with water.

$$CaC_2 + 2H_2O = Ca(OH)_2 + C_2H_2\uparrow \quad (1)$$

$$CaC_2 + H_2O = CaO + C_2H_2\uparrow \quad (2)$$

$$CaC_2 + H_2O = CaO + 2C + H_2\uparrow \quad (3)$$

In this study, we managed to synthesize highly crystalline few-layer graphene (FLG) at room temperature (RT, 20–25 °C) through the redox chemistry of tetragonal-phased CaC_2 with water. The water-assisted RT-synthesized carbon from CaC_2 was revealed to possess 2–5 layers and was highly graphitic (containing >93 at% carbon). A rational mechanism was proposed: C_2^{2-} anions donate their electrons to nearby oxidative H^+ in H_2O, followed by topotactic coupling of C≡C dumbbells to form a conjugated sp^2-carbon network. The redox chemistry and mutual cross-linking of C_2^{2-} anions were further evidenced by CaC_2 reacting with non-volatile metal cations such as Ag^+, which resulted in a larger amount of graphitic carbon materials and small sized Ag nanoparticles. We believe that this mild redox chemistry strategy is applicable for the synthesis of many other layered inorganic elementary substances such as phosphorene and borophene from metal compounds embedded with pre-structured P or B anions.

2. Results and discussion

Few-layered graphene (FLG) was obtained *via* simple dropwise addition of water onto CaC_2 powder. A large amount of acetylene was generated once CaC_2 came into contact with water, as can be seen from the evident volume change after the addition of the first drop of water (Fig. 1A-a/b). The high reaction intensity is mainly because of its very low Gibbs free energy ($\Delta G_m^\theta = -35.7$ kJ mol^{-1}) and fast removal of acetylene into open air. Our interest is in the CaC_2 reaction with water to form carbon and hydrogen, and the Gibbs free energy of this specific reaction is −86.6 kJ mol^{-1}, which is even more thermodynamic.

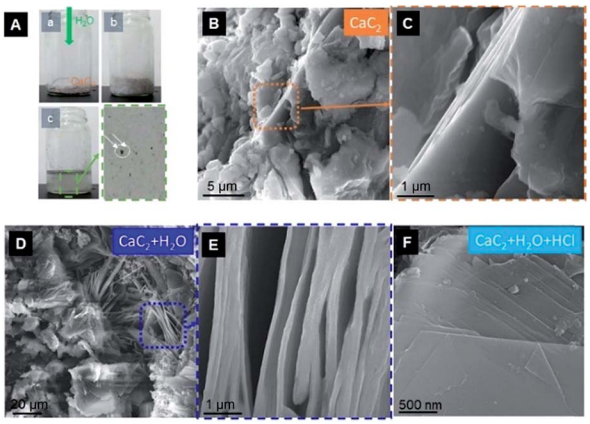

Fig. 1 (A) Digital images of CaC_2 reaction with water: (a) addition of one drop of water to CaC_2 powder; (b) intensive reaction between CaC_2 and water, generating C_2H_2; and (c) further addition of water to enable full reaction of CaC_2, resulting in black materials, as marked in the enlarged area in (c). (B) Typical SEM image of pristine CaC_2, partial enlargement in (C) reveals the sharp edges of crystalline CaC_2. (D) SEM image of the unwashed product from the reaction of CaC_2/H_2O, the enlarged area in (E) reveals the expanded layered structure. (F) SEM image of the acid-washed product from the reaction of CaC_2/H_2O, revealing a typical layered form.

However, currently, there is no report on formation of carbon from CaC_2 at conventional temperature and pressure.[18,35] We assumed that this is mainly because of the highly competitive kinetics of fast generation and removal of acetylene relative to that of carbon/hydrogen formation. After the reaction was fully stopped by adding excess water, diluted HCl was used to remove $Ca(OH)_2$ and other metallic impurities. After acid washing, the black product can be clearly observed and it becomes obvious in the enlarged view shown in Fig. 1A-c despite the low yield.

SEM characterization was performed to reveal the morphology of the CaC_2 precursor and the resultant of CaC_2/H_2O reaction before and after acid washing. Fig. 1B shows the typical irregularly shaped polycrystalline morphology of CaC_2, and the enlarged view (Fig. 1C) indicates the existence of sharp edges. After the reaction was completed, grey powder containing carbon (black) and a large amount of $Ca(OH)_2$ (white) was collected using centrifugation and washed with water. Fig. 1D exhibits the morphology of the product derived from CaC_2/H_2O reaction, indicating a typical layered form, which is completely different from that of the CaC_2 precursor. Meanwhile, the adjacent layers are found to be separated by interspaces, as typified in Fig. 1E. Then, the grey resultant was submitted to acid washing using 10 wt% HCl. Fig. 1F shows the typical SEM image of the acid-washed resultant, revealing stacked sheets with intact layers and clear edges.

Thereafter, XRD measurements were used to confirm the phase of the layered resultant. Fig. 2A shows its typical XRD profile, revealing a pointed diffraction peak located at ~26.5° that can be assigned to the (002) peak of graphitic carbon (PDF # 65-6212). The XRD profile of precursor CaC_2 was also recorded; as shown in Fig. 2A, no sign of graphitic carbon was detected, indicating that the CaC_2 precursor is free of FLG or graphite.[37] We further tested a series of experimental conditions to confirm

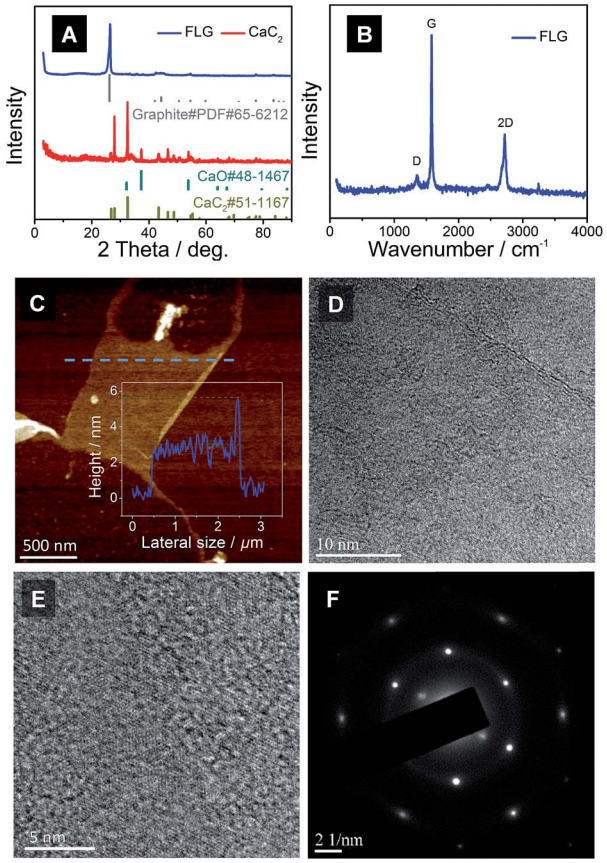

Fig. 2 (A) XRD profiles and (B) displays the Raman spectra of FLG. (C) AFM image of FLG, the inset shows the thickness of FLG. (D) Typical HRTEM image of FLG displaying clean edges. (E) Enlargement of basal planes of FLG shows the hexagonal close-packed carbon atoms. (F) Electron diffraction pattern of FLG.

that CaC_2 is free of graphitic carbon. It was found that milling CaC_2 with LiOH did not result in layered carbonaceous materials after acid wash (Fig. S1†), further evidencing that the FLG was indeed converted from CaC_2. The minor inclusion of CaO is probably due to the oxidation occurring during XRD measurement in air. Fig. 2B displays the Raman spectra of FLG. A sharp and strong band (G band) located at ~1583 cm^{-1} can be assigned to the stretching mode of the conjugated C=C bond, which clearly indicates the high graphitization degree of FLG.[38,39] The band located at ~1352 cm^{-1} is attributed to the disordered breathing mode of the conjugated carbon ring; the very low intensity of this band (D band) indicates that a very low defect content is present in FLG.[40] The apparent 2D band (an overtone band) at ~2700 cm^{-1} relative to the G band confirms that the obtained graphene is few layered.[41]

Fig. 2C exhibits the atomic force microscopy (AFM) image of FLG after dispersion and sonication in DMF, revealing an approximate thickness of 2.7 nm. In the enlarged HRTEM image of the edges of the selected FLG sheet, 2–3 layered FLG is revealed (Fig. 2D). Further magnification clearly displayed the intact hexagonal close packing of carbon atoms (Fig. 2E). The electron diffraction pattern of the selected area of FLG was recorded; as shown in Fig. 2F, hexagonal-patterned bright dots are revealed, confirming that FLG has a single-crystalline phase. XPS characterization was performed to further reveal the composition of FLG. The XPS elemental survey shown in Fig. 3A reveals the presence of three main types of elements: C, O, and S in FLG; remarkably, its carbon content reaches up to 92.2 at%. The doping of S and O heteroatoms was possibly due to the S impurities in CaC_2 and air, respectively.[33] Deconvoluted XPS C 1s spectra indicate that the carbon atoms are overwhelmingly involved in C–C and C=C bonding, which supports that FLG is highly graphitized and agrees with the information from HRTEM and XRD analysis.

In order to shed light on the conversion mechanism of CaC_2 to FLG, we submitted the gaseous by-products to gas chromatography (GC) measurements. Fig. 3C shows the typical GC results, revealing three kinds of gaseous products, methane, ethylene, and hydrogen, along with the overwhelming acetylene production. The concentration of hydrogen under normal temperature and pressure can reach up to ~84 ppm, which supports that the FLG is probably obtained *via* eqn (3). The other two gaseous products formed were methane and ethylene. The generation of a minor amount of ethylene may be attributed to the deep hydrogenation during the fast formation of graphitic carbon. Methane was probably formed by the hydrogenation of dangling carbon species instead of complete C_2^{2-} anions. More interestingly, by simply using aqueous media with different H^+ strengths (NaCl solution, pure water, and diluted HCl), we found that the element contents of the resulting FLG could be largely varied (Fig. 3D). For instance, the carbon content of FLG obtained using NaCl solution is 96.95 at%, which decreased to 93.45 at% when using pure water, and further decreased to 91.44 at% when using HCl, which is possibly correlated with reaction intensity. Meanwhile, the impurities from the CaC_2 precursor and oxygen from air potentially serve as dopants to achieve N, S, and O doping. The heteroatom doping level including N, S, and O kept increasing

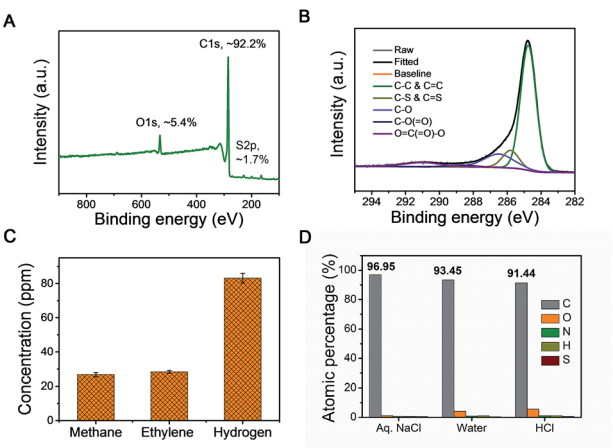

Fig. 3 (A) XPS survey and (B) XPS C 1s spectra of FLG. (C) Gas chromatography results of the gaseous products from the reaction of CaC_2 and water, revealing the presence of methane, ethylene, and hydrogen in addition to a massive amount of acetylene. (D) Organic elemental analysis of FLG materials obtained using different aqueous solutions: saturated NaCl solution, pure water, and diluted HCl solution (10 wt%).

in sequence of using NaCl solution, pure water, and diluted HCl, which proved our hypothesis that the H^+ strength determined the effectiveness of C–C coupling during the redox chemistry.

Furthermore, it was found that water could be substituted by other H-containing agents such as acetic acid and ethylene glycol to convert CaC_2 into FLG. As shown in Fig. S2,† the FLG converted using acetic acid and ethylene glycol seemingly contains fewer layers as revealed by its more flexible texture. However, the reaction rates and yields are largely varied. Remarkably, acetic acid-promoted synthesis of FLG showed a Raman I_{2D}/I_G ratio of ~0.94 (Fig. S3†), revealing that FLG is present as a single layer or bi-layer. However, its defect level, as indicated in Fig. S3,† is also intensified, reaching a Raman I_D/I_G ratio of ~0.22 relative to 0.07 of FLG obtained from reaction with water. Meanwhile, the yields of FLG obtained using different H-containing solvents or solutions exhibited large differences, and a rough conclusion can be drawn that a higher amount of FLG will be obtained if using solvent with higher H activity (Table S1†). Fig. 4A reveals that, besides the presence of flat few-layer graphene, a few crumpled FLG sheets are observable, which are seemingly templated by solid particles. We assumed that the graphitic carbon with voids was mainly formed by the slow removal of Ca^{2+} from the *in situ* formed graphene interlayer. In the meantime, the slow rate of Ca^{2+} exclusion from the C≡C coupling plane does not allow the as-formed graphene layers to stack easily relative to that in aqueous media, in turn, resulting in more single-layer and bi-layer graphene sheets. The electron diffraction pattern (inset of Fig. 4A) reveals that these FLG sheets obtained *via* acetic acid reaction are no longer single-crystalline but polycrystalline, as indicated by the dispersive dots in the hexagonal layout, also confirming their relatively high defect content. For the acetic acid-promoted FLG synthesis, using simple re-dispersion and sonication in NMP can enable the fabrication of low-defect large-area graphene sheets, as shown in Fig. 4B and the SEM image in Fig. S4A in the ESI.† We noticed that the upper layer of FLG suspension resulted in more single-layer or bi-layer graphene sheets but more defective graphene sheets were also detected by Raman spectroscopy (Fig. S4B†).

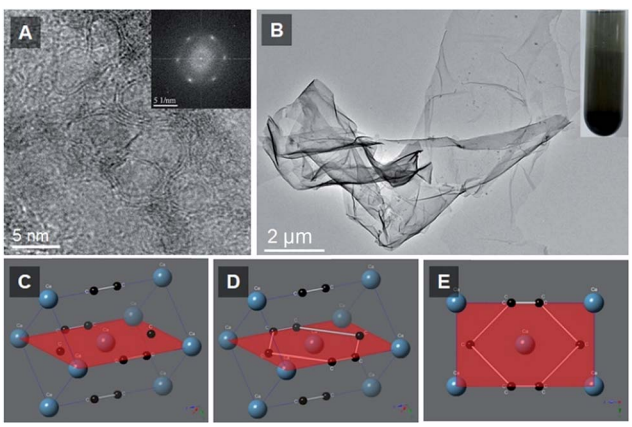

Fig. 4 (A) HRTEM image of upper-layer FLG, crumpled graphene layers are observable, the inset shows the typical electron diffraction pattern of the upper-layer FLG. (B) TEM image of FLG after re-suspension and centrifugation, the inset shows the gradient FLG suspension after centrifugation at 1000 rpm for 1 min. (C) Crystal structure of the CaC_2 unit structured by Ca^{2+} nodes and C_2^{2-} linkers. (D) The formation of an aromatic six-atom carbon ring by possible C_2^{2-} cross-linking. (E) Perpendicular view of the basal plane of the carbon ring pre-occupied in CaC_2 lattices.

To shed light upon the deep conversion mechanism, the crystal structure of CaC_2 was investigated. As shown in Fig. 4C, a crystal plane consisting of central Ca^{2+} nodes and a C≡C framework is displayed.[34] Probably, adjacent C≡C bonds readily connect with each other to form an aromatic six-membered carbon ring once the excessive electrons in C_2^{2-} anions were extracted by oxidative species.[42] In the meantime, Ca^{2+} in the centre would be excluded from the basal plane (Fig. 4D/E). Previous reports have demonstrated that CaC_2 is capable of functioning as a powerful reducing agent at temperatures above 800 °C.[36] Considering its high reduction potential, it is reasonable to explain that CaC_2 can function as a mild agent to reduce oxidative species or agents under mild conditions, for instance, normal temperatures and pressures in our cases with H-containing molecules. Once the electrons are transferred from C_2^{2-} to adjacent oxidative species *via* redox routes, neutralized C≡C would approach each other and undergo coupling. Due to the pre-embedded hexagonal layout of carbon atoms in the same plane, aromatic carbon rings would be dynamically formed.[42] In the meantime, in-plane Ca^{2+}, free of electrostatic force confinement, will be ejected from the six-atom carbon ring plane.

Furthermore, we promoted the more efficient crosslinking of C_2^{2-} by using oxidative non-volatile metallic cations. The inset of Fig. S5A in the ESI† shows the black ink resulting from the CaC_2 reaction with $AgNO_3$, which typifies a much larger quantity of the black product relative to that of the CaC_2/H_2O reaction. The SEM image (Fig. S5A†) shows the formation of typical layered materials. XRD characterization confirmed that the black product after water washing contained the Ag substance (Fig. S5B in the ESI†). In contrast to the H_2O oxidation agent, Ag^+ provides higher oxidation potential to match the reductive CaC_2; also, the fixable metallic cations do not allow the C≡C (after electron depletion of C_2^{2-}) to vaporize or leave the reaction system. Therefore, it is more feasible to produce graphene from CaC_2 *via* redox reaction with metal cations.

3. Experimental section

3.1 Materials

Calcium carbide (grade 1) was obtained from Aladdin Chemical Co., Ltd. $AgNO_3$, *N*-methyl pyrrolidone (NMP), acetic acid, ethylene glycol, and sodium chloride (NaCl) were of A.R. grade, and were purchased from Beijing Chemical Works and used as received. Concentrated HCl (35.0 wt%) was also purchased from Beijing Chemical Works.

3.2 Preparation of graphene from CaC_2

Typically, fine CaC_2 powder was obtained by hand grinding bulk CaC_2 under the protection of N_2 gas. 1.00 g of CaC_2 powder was

placed in a transparent vial, followed by drop-wise addition of 5.0 mL deionized water. After the reaction was fully stopped, 10.0 mL diluted HCl (10 wt%) was added to the vial. The vial was sonicated to fully remove insoluble Ca compounds and any impurity. The black product was further washed with deionized water, collected using centrifugation, and eventually dried at 80 °C in ambient air. For comparison, other H-containing solvents including diluted HCl, acetic acid, and ethylene glycol were selectively used to investigate the effect of variation of H^+ strength on the synthesis of graphene. In order to exclude the pre-embedded graphite impurity in the CaC_2 source, a control experiment of CaC_2 grinding with LiOH was set up in air. Control experiments of reducing Ag^+ by CaC_2 were set by substituting deionized water with 0.1 mol L^{-1} $AgNO_3$/NMP solution. The as-resulted black materials were thoroughly washed with water and dried at 80 °C.

3.3 Characterization

Scanning electron microscopy (SEM, operated at 20 kV) images were recorded using a Zeiss SUPRA 55. High-resolution transmission electron microscopy (HRTEM, operated at 200 kV) images were recorded using a JEOL 2100 high-resolution transmission electron microscope. Atomic force microscopy (AFM) images were obtained on a Bruker scanning probe microscope (DMFASTSCAN2-SYS). Raman spectra were recorded on a LabRAM Aramis Raman spectrometer (HORIBA Jobin Yvon, 400–4000 cm^{-1}). Powder X-ray diffraction (XRD) patterns were recorded on an X-ray diffractometer (MeasSrv F9XDZ42) at a scan rate of 10 °C min^{-1} in the 2θ range of 5 to 80°. X-ray photoelectron spectroscopy (XPS) was carried out on a Thermo Electron ESCALAB250 XPS spectrometer. Organic elemental analysis (OEA) of H, C, N, and O elements was performed on a Flash EA 1112 elemental analyser. Thermogravimetric analyses (TGA) were performed on a Pyris Diamond TG instrument (HCT-1). Resistance analyses were carried out on an RTS-4 four-probe meter. A GC (SHIMADZU GC-2014) with an automatic injection system was used to analyse the composition of gas products.

4. Conclusions

In summary, for the first time, we managed to fabricate highly crystalline few-layered graphene (FLG) from commercialized CaC_2. The fabrication process was carried out under mild conditions: reaction with water, room temperature (RT, 20–25 °C) and normal pressure. The water-assisted RT synthesized FLG from CaC_2 was revealed to be highly graphitized and of ~3 nm thickness, containing >93 at% carbon. A rational mechanism was proposed: C_2^{2-} anions donate their electrons to nearby oxidative species, for instance, H^+ in water, followed by topo-tactically self-coupling to form a conjugated sp^2-carbon network. Furthermore, more efficient FLG synthesis was developed by using non-volatile Ag^+ as the oxidative agent, which was evidenced by the formation of a larger amount of black product and small sized Ag nanoparticles. We believe that this mild topotactic conversion of CaC_2 into graphene is promising for the synthesis of other layered inorganic elementary substances such as phosphorene and borophene from metal compounds embedded with pre-structured P or B anions.

Conflicts of interest

There are no conflicts to declare.

Acknowledgements

This work was financially supported by the National Natural Science Foundation of China (NSFC, 21520102002, 91622116, 21471014, and 21701101), the National Key Research and Development Project (2016YFF0204402), the Fundamental Research Funds for the Central Universities, the Long-Term Subsidy Mechanism from the Ministry of Finance and the Ministry of Education of PRC, the Shandong Scientific Research Awards Foundation for Outstanding Young Scientists (grant number ZR2018JL010), and the Shandong Joint Fund of Outstanding Young Talents (grant number ZR2017BB018). We also thank the Scientific Research Foundation of the Shandong University of Science and Technology for Recruited Talents (grant number 2017RCJJ059).

References

1 J. N. Coleman, *Acc. Chem. Res.*, 2013, **46**, 14–22.
2 W. Ren and H. M. Cheng, *Nat. Nanotechnol.*, 2014, **9**, 726–730.
3 Y. Wu, B. Wang, Y. Ma, Y. Huang, N. Li, F. Zhang and Y. Chen, *Nano Res.*, 2010, **3**, 661–669.
4 M. I. Kairi, S. Dayou, N. I. Kairi, S. A. Bakar, B. Vigolo and A. R. Mohamed, *J. Mater. Chem. A*, 2018, **6**, 15010–15026.
5 Y. Anno, Y. Imakita, K. Takei, S. Akita and T. Arie, *2D Mater.*, 2017, **4**, 025019.
6 Z. Xu, Y. Liu, X. Zhao, L. Peng, H. Sun, Y. Xu, X. Ren, C. Jin, P. Xu and M. Wang, *Adv. Mater.*, 2016, **28**, 6449–6456.
7 B. Dai, L. Fu, L. Liao, N. Liu, K. Yan, Y. Chen and Z. Liu, *Nano Res.*, 2011, **4**, 434–439.
8 K. S. Novoselov, A. K. Geim, S. V. Morozov, D. Jiang, Y. Zhang, S. V. Dubonos, I. V. Grigorieva and A. A. Firsov, *Science*, 2004, **306**, 666–669.
9 N. I. Kovtyukhova, Y. Wang, A. Berkdemir, R. Cruz-Silva, M. Terrones, V. H. Crespi and T. E. Mallouk, *Nat. Chem.*, 2014, **6**, 957–963.
10 K. R. Paton, E. Varrla, C. Backes, R. J. Smith, U. Khan, A. O'Neill, C. Boland, M. Lotya, O. M. Istrate and P. King, *Nat. Mater.*, 2014, **13**, 624–630.
11 M. Choucair, P. Thordarson and J. A. Stride, *Nat. Nanotechnol.*, 2009, **4**, 30–33.
12 D. Li, M. B. Müller, S. Gilje, R. B. Kaner and G. G. Wallace, *Nat. Nanotechnol.*, 2008, **3**, 101–105.
13 X. H. Xia, D. L. Chao, Y. Q. Zhang, Z. X. Shen and H. J. Fan, *Nano Today*, 2014, **9**, 785–807.
14 X. Xu, Z. Zhang, L. Qiu, J. Zhuang, L. Zhang, H. Wang, C. Liao, H. Song, R. Qiao and P. Gao, *Nat. Nanotechnol.*, 2016, **11**, 930–935.

15 S. Xiang, V. Miseikis, L. Planat, S. Guiducci and S. Roddaro, *Nano Res.*, 2016, **9**, 1823–1830.
16 L. Jiang, T. Niu, X. Lu, H. Dong, W. Chen, Y. Liu, W. Hu and D. Zhu, *J. Am. Chem. Soc.*, 2013, **135**, 9050–9054.
17 X. Zou, L. Ji, H.-Y. Hsu, K. Zheng, Z. Pang and X. Lu, *J. Mater. Chem. A*, 2018, **6**, 12724–12732.
18 J. Fischer, W. Zhou, Y. Gogotsi, A. Nikitin, H. Ye, M. Barsoum, B. Yi and H. Foley, *Nat. Mater.*, 2003, **2**, 591–594.
19 R. K. Dash, A. Nikitin and Y. Gogotsi, *Microporous Mesoporous Mater.*, 2004, **72**, 203–208.
20 G. N. Yushin, E. N. Hoffman, A. Nikitin, H. Ye, M. W. Barsoum and Y. Gogotsi, *Carbon*, 2005, **43**, 2075–2082.
21 X. Li, X. Pan, L. Yu, P. Ren, X. Wu, L. Sun, F. Jiao and X. Bao, *Nat. Commun.*, 2014, **5**, 3688.
22 P. Simon, X. J. Feng, M. Bobnar, P. Höhn, U. Schwarz, W. Carrillocabrera, M. Baitinger and Y. Grin, *ACS Nano*, 2017, **11**, 1455–1465.
23 N. Tian, Y. Gao, Y. Li, Z. Wang, X. Song and L. Chen, *Angew. Chem., Int. Ed.*, 2016, **55**, 644–648.
24 Z. Kou, T. Meng, B. Guo, I. S. Amiinu, W. Li, J. Zhang and S. Mu, *Adv. Funct. Mater.*, 2016, **27**, 1604904.
25 C. Dai, X. Wang, W. Ying, L. Na and J. Wei, *Mater. Chem. Phys.*, 2008, **112**, 461–465.
26 H. Schobert, *Chem. Rev.*, 2014, **114**, 1743–1760.
27 K. S. Rodygin, G. Werner, F. A. Kucherov and V. P. Ananikov, *Chem.–Asian J.*, 2016, **11**, 965–976.
28 R. C. Pillai, E. M. Sabolsky, S. L. Rowan, I. B. Celik and S. Morrow, *Ind. Eng. Chem. Res.*, 2015, **54**, 11001–11010.
29 H. Zheng, L. Wang, K. Li, Y. Yang, Y. Wang, J. Wu, X. Dong, C.-H. Wang, C. A. Tulk and J. J. Molaison, *Chem. Sci.*, 2017, **8**, 298–304.
30 J. Nylén, S. Konar, P. Lazor, D. Benson and U. Häussermann, *J. Chem. Phys.*, 2012, **137**, 115.
31 L. Wang, X. Huang, D. Li, Y. Huang, K. Bao, F. Li, G. Wu, B. Liu and C. Tian, *J. Chem. Phys.*, 2016, **144**, 194506.
32 L. Wang, X. Dong, Y. Wang, H. Zheng, K. Li, X. Peng, H.-k. Mao, C. Jin, Y. Meng, M. Huang and Z. Zhao, *J. Phys. Chem. Lett.*, 2017, **8**, 4241–4245.
33 H. Klaus, K. Alfons, M. Bernd and S. Josef, *Calcium Carbide*, Wiley-VCH Verlag GmbH & Co. KGaA, 2000.
34 N.-G. Vannerberg, *Acta Chem. Scand.*, 1961, **16**, 1212–1220.
35 F. E. Caropreso, PhD thesis, Seton Hall University, 1969.
36 D. Lindström and S. Du, *Metall. Mater. Trans. B*, 2015, **46**, 83–92.
37 S. Konar, J. Nylén, G. Svensson, D. Bernin, M. Edén, U. Ruschewitz and U. Häussermann, *J. Solid State Chem.*, 2016, **239**, 204–213.
38 S. Pei and H.-M. Cheng, *Carbon*, 2012, **50**, 3210–3228.
39 Y. Hernandez, V. Nicolosi, M. Lotya, F. M. Blighe, Z. Sun, S. De, I. McGovern, B. Holland, M. Byrne and Y. K. Gun'Ko, *Nat. Nanotechnol.*, 2008, **3**, 563–568.
40 C. Casiraghi, S. Pisana, K. S. Novoselov, A. K. Geim and A. C. Ferrari, *Appl. Phys. Lett.*, 2007, **91**, 183.
41 P. H. Tan, W. P. Han, W. J. Zhao, Z. H. Wu, K. Chang, H. Wang, Y. F. Wang, N. Bonini, N. Marzari and N. Pugno, *Nat. Mater.*, 2012, **11**, 294–300.
42 S. M. Pratik, A. Nijamudheen and A. Datta, *Chem.–Eur. J.*, 2015, **21**, 18454–18460.